# HARNESSING THE POTENTIAL OF DENDRITIC CELL-DERIVED EXOSOMES AS TOOLS FOR IMMUNOTHERAPY IN OVARIAN CANCER

A Thesis

by

YAJAIRA SOFIA JIMENEZ

Submitted to the Graduate and Professional School of
Texas A&M University
in partial fulfillment of the requirements for the degree of

MASTER OF SCIENCE

| | |
|---|---|
| Chair of Committee, | David P. Huston |
| Committee Members, | Bruna Corradetti |
| | Rajesh C. Miranda |
| Head of Program, | Carol M. Vargas Bautista |

May 2022

Major Subject: Medical Sciences

ABSTRACT

Ovarian cancer is the second most common gynecologic cancer in the United States. Part of what makes ovarian cancer so deadly is its ability to steadily grow in the peritoneum undetected until it reaches advanced stages. Therapies used to treat ovarian cancer include debulking surgery and platinum-based chemotherapy, but even after undergoing this treatment, there is a 70% remission rate. Current studies show that using dendritic cells for T cell activation can be a useful approach to prime our immune system against tumor cells in efforts to increase survival rate and decrease relapses. Although immunotherapy is a promising cancer treatment method, it fails to have an impact on patients with advanced ovarian cancer due to the immunosuppressive and heterogeneous micro-environment and impaired lymphatic drainage created by cancer cells within the peritoneal cavity. We are interested in boosting the anti-tumor immunity by employing exosomes derived from dendritic cells (DC)-based vaccines (Dex) for their capacity of overcoming the transport barriers, bypassing the immunosuppressive environment, prompting T cell infiltration in target organs, and activating them. To address this, we have specifically activated DCs and evaluate the potential of Dex to induce an anti-tumor immune response in vitro. Once adequate activation was achieved, in vivo studies using a metastatic ovarian cancer model available at Corradetti Lab (HMRI) have been used to determine biodistribution of the Dex using various injection routes.

ACKNOWLEDGEMENTS

Thank you to the members of my committee, Dr. Corradetti, Dr. Huston, Dr. Miranda for their guidance and support throughout the course of this research. To my mentors Dr. Bruna Corradetti and Dr. Huston who were essential to my growth as a physician-scientist this year. To my friends and family. Mom, dad, Alex, Jose, Andrew thanks for always being a phone call away, for your encouragement, patience, and love. To the people in the department who took me under their wing and were there for me throughout this experience. It takes a village, and this thesis would have not been possible without all your help!

CONTRIBUTORS AND FUNDING SOURCES

## Contributors

The student contributed to an existing project conceived by Dr. Corradetti and under development in the Corradetti lab at HMRI. The thesis committee consisting of Dr. Bruna Corradetti, Dr. Huston, and Dr. Miranda discussed the results obtained by the student that represent part of this work.

## Funding Sources

The project was partially supported by Golfers Against Cancer in 2018 to Dr. Corradetti. Yajaira Jimenez is a Burrow Wellcome Fund Scholar supported by a Burroughs Wellcome Fund Scientist Institutional Award to the Texas A&M University Academy of Physician Scientists.

## NOMENCLATURE

| | |
|---|---|
| OC | Ovarian Cancer |
| DC | Dendritic cell |
| DC-A | Activated Dendritic cell |
| DC-AO | Activated/Ovalbumin Dendritic cell |
| Dex | Dendritic cell-derived exosomes |
| Dex-A | Activated Dendritic cell-derived exosomes |
| De-AO | Activated/Ovalbumin Dendritic cell-derived exosomes |
| NTA | Nanoparticle Tracking Analysis |
| IVIS | In-Vivo Imaging System |
| IV | Intravenous |
| IP | Intraperitoneal |

TABLE OF CONTENTS

Page

LIST OF FIGURES

Page

# 1. INTRODUCTION

## 1.1. CELL-FREE IMMUNOTHERAPY

Bioactive cells (i.e. stem cells and immune cells, such as dendritic cells, DCs) are crucial in supporting body's homeostasis and are required for the body's line of defense against external harmful factors and tumor initiation. They achieve this mission through communication with surrounding cells, through the release of paracrine signals (including diffusible factors and extracellular vesicles) making them a powerful tool for development of therapeutics in regenerative medicine and oncology.[1] While the clinical application of cell-based approaches is promising, their use is hindered by challenges associated to the fact that 1) bioactive cells may lose their therapeutic potential when exposed to immunosuppressive microenvironments, 2) batch-to-batch variability, 3) need for large amount of cells to develop therapeutics, and 4) difficulties in long-term storage without cell damage and propensity for cell anergy.[2,3] In this context, exosomes, which are vesicles released by cells as means for communication with cells located in surrounding and distant districts in the body, have gained fame as cell-free alternatives. They offer advantages over the use of their parental cells due to 1) shared receptors which allow them to target and activate specific cell types directly through antigen presentation or by cross-dressing and merging into their plasma membrane, 2) the nanoscopic size (in the range of 150-300 nm) which supports an easier tissue penetration and improved biodistribution[3], 3) their bioactive status is not susceptible of the negative effect exerted by the environment 4) scale-up opportunities in the manufacturing

process, and 5) the possibility to be stored at low temperatures for prolonged periods of time without losing their effectiveness.

Exosomal therapy has already been successfully used as a cell-free alternative in melanoma and cervical cancer murine animal models resulting in tumor reduction and progression-free survival.[4,5] However, use of this therapy in ovarian cancer presents a unique hurdle due to its classification as a "cold" tumor based on low tumor mutational burden and low T cell–inflamed gene expression profile.[6]

## 1.2. THE TUMOR MICROENVIRONMENT

The tumor microenvironment is essential in cancer promoting or cancer suppressive actions by the immune system and is often the limiting factor in immune cell infiltration in the tumor and successful immunotherapy.[7,8] Tumors have been classified as being "cold" (noninflamed), "hot" (inflamed) or "immunoexcluded" (immune cells found mostly at the border of the tumor).[7,9] This classification is a helpful predictor of therapeutic since the environment can prove to be a barrier for therapies relying on increasing T cell immune responses against tumor cells since they might not present with desired outcomes based on the relative lack of immune cell penetration and ability to be activated to mount a response.[10]

In fact, ovarian cancer tumors found to have increased numbers of intertumoral T cells had a statistically significant increase in survival even with suboptimal debulking surgery when compared to patients without intertumoral T cells – highlighting the importance of proper T cell activation and tumor infiltration for good treatment response.[11]

## 1.3. UNIQUE CHALLENGES AND USE OF ADJUVANTS

Dex have been proven to activate T cells in various studies but are continuously suboptimal in CTL activation when compared to their progenitor cells.[4,12] One reason could be the need for multiple immune cell activators including immature DC to correctly activate Dex when presented antigen.[13,14] This, coupled with the "cold" tumor microenvironment found in ovarian cancer may be the reason behind the limited therapeutic benefits Dex vaccines have had in the past.[4] Proper immune response might prove to be difficult in a tumor environment containing exhausted inflammatory cells such as the one found in ovarian cancer.[10] Therefore, use of adjuvants in Dex vaccines such as Poly (I:C) might improve treatment outcomes by increasing inflammation through activation of both innate and adaptive immune cells through natural killer cell and TLR3 receptor activation respectively.[4] Dex treatment with poly(I:C) has shown promising results in treatment of melanoma and cervical cancer in murine animal models.[4,5] We postulate that the addition of Poly(I:C) as an adjuvant in the pulsing of DC with OC whole tumor antigen will lead to improved immunogenicity of cells and enhance treatment potential in our murine advanced ovarian cancer model.

## 1.4. REFERENCES

1. Chen, D. S., & Mellman,I. (2013). Oncology Meets Immunology: The Cancer-Immunity Cycle. Immunity, 39(1), 1–10. https://doi.org/10.1016/j.immuni.2013.07.012

2. Nikfarjam, S., Rezaie, J., Kashanchi, F., & Jafari, R. (2020). Dexosomes as a cell-free vaccine for cancer immunotherapy. Journal of Experimental & Clinical Cancer Research, 39(1). https://doi.org/10.1186/s13046-020-01781-x

3. Pitt, J. M., André, F., Amigorena, S., Soria, J.-C., Eggermont, A., Kroemer, G., & Zitvogel, L. (2016). Dendritic cell–derived exosomes for cancer therapy. Journal of Clinical Investigation, 126(4), 1224–1232. https://doi.org/10.1172/jci81137

4. Damo, M., Wilson, D. S., Simeoni, E., & Hubbell, J. A. (2015). TLR-3 stimulation improves anti-tumor immunity elicited by dendritic cell exosome-based vaccines in a murine model of melanoma. *Scientific Reports, 5*(1). doi:10.1038/srep17622

5. Chen, S., Lv, M., Fang, S., Ye, W., Gao, Y., & Xu, Y. (2018). Poly(I:C) enhanced anti-cervical cancer immunities induced by dendritic cells-derived exosomes. *International Journal of Biological Macromolecules, 113*, 1182-1187. doi:10.1016/j.ijbiomac.2018.02.034

6. Cristescu, R., Mogg, R., Ayers, M., Albright, A., Murphy, E., Yearley, J., . . . Kaufman, D. (2018). Pan-tumor genomic biomarkers for PD-1 checkpoint blockade–based immunotherapy. *Science, 362*(6411). doi:10.1126/science.aar3593

7. Kather, J. N., Suarez-Carmona, M., Charoentong, P., Weis, C., Hirsch, D., Bankhead, P., . . . Halama, N. (2018). Topography of cancer-associated immune cells in human solid tumors. *ELife, 7*. doi:10.7554/elife.36967

8. Preston, C. C., Goode, E. L., Hartmann, L. C., Kalli, K. R., & Knutson, K. L. (2011). Immunity and immune suppression in human ovarian cancer. *Immunotherapy*, *3*(4), 539–556. https://doi.org/10.2217/imt.11.20

9. Corradetti, B., Pisano, S., Conlan, R. S., & Ferrari, M. (2019). Nanotechnology and Immunotherapy in Ovarian Cancer: Tracing New Landscapes. *Journal of Pharmacology and Experimental Therapeutics, 370*(3), 636-646. doi:10.1124/jpet.118.254979

10. Nizzero, S., Shen, H., Ferrari, M., & Corradetti, B. (2020). Immunotherapeutic Transport Oncophysics: Space, Time, and Immune Activation in Cancer. *Trends in Cancer, 6*(1), 40-48. doi:10.1016/j.trecan.2019.11.008

11. Zhang, L., Conejo-Garcia, J. R., Katsaros, D., Gimotty, P. A., Massobrio, M., Regnani, G., . . . Coukos, G. (2003). Intratumoral T Cells, Recurrence, and Survival in Epithelial Ovarian Cancer. *New England Journal of Medicine,348*(3), 203-213. doi:10.1056/nejmoa020177

12. Ju, X., Zhang, H., Zhou, Z., & Wang, Q. (2020). Regulation of PD-L1 expression in cancer and clinical implications in immunotherapy. *American journal of cancer research*, *10*(1), 1–11.

13. Näslund, T. I., Gehrmann, U., Qazi, K. R., Karlsson, M. C., & Gabrielsson, S. (2013). Dendritic Cell–Derived Exosomes Need To Activate Both T and B Cells To Induce Antitumor Immunity. *The Journal of Immunology, 190*(6), 2712-2719. doi:10.4049/jimmunol.1203082

14. André, F., Chaput, N., Schartz, N. E., Flament, C., Aubert, N., Bernard, J., . . . Zitvogel, L. (2004). Exosomes as Potent Cell-Free Peptide-Based Vaccine. I. Dendritic Cell-Derived Exosomes Transfer Functional MHC Class I/Peptide Complexes to Dendritic Cells. *The Journal of Immunology, 172*(4), 2126-2136. doi:10.4049/jimmunol.172.4.2126

## 2. CHARACTERIZATION OF CELLULAR AND EXOSOMAL ISOLATES

Dendritic cells are antigen-presenting cells that prime the immune system against foreign invaders allowing researchers to develop cell-based vaccines to enable targeted activation. The first step in creating an adequate vaccine was obtaining good maturation and activation of dendritic cells (DCs) from bone-marrow hematopoietic stem cells. We used the markers MHC-II and CD11c to evaluate proper maturation into a monocytic lineage and upregulation of co-stimulatory markers (CD80 and CD86) to show activation of dendritic cells.[1,2]

After isolation of exosomes, a comprehensive quality control process is required to ensure that specific and functional signatures are retained on the membrane of exosomal preparations. Although no "gold standard" for exosomal receptor characterization exists, the International Society for Extracellular Vesicles (ISEV) provides guidelines on single vesicle analysis using direct visualization through flow cytometry or electron microscopy or by calculating biophysical parameters through Nanoparticle Tracking Analysis (NTA).[3] We also used western blotting analysis to show the presence of membrane proteins (Alix, TSG 101) and fusion proteins (CD9) in the isolates we collected.[4]

While single vesicle analysis through direct visualization is achievable for large extracellular vesicles, such as microvesicles (up to 1 micron in size), flow cytometry size restrictions do not allow for direct identification of specific exosomal populations of exosomes outside calculation of biophysical parameters unless they are conjugated to microscopic beads, curbing this limitation.[5] Bead-assisted flow cytometry allows for the

detection and quantification of surface markers on exosomes by allowing the user to gate the exosomal population based on bead size.

Aldehyde-sulfate latex beads are a popular choice since they do not restrict binding based on exosomal receptors, allowing for most of the exosomal surface to be exposed to the antibody of interest.[6] However, while processing our samples we realized that antibody aggregates and false positives hamper a comprehensive characterization of the exosomal preparations. These observations had been previously described by Suarez et al. dependent on antibody absorption on the bead surface, introducing potential setbacks with this method of receptor quantification.[6] We qualified the exosomes using this method by utilizing the ImageStream machine to allow for direct visualization of the beads and fluorescence reading allowing us to reduce the number of false positives we were obtaining due to the setbacks mentioned above.

## 2.1. METHODS

### 2.1.1. Bone marrow-derived Dendritic Cell Culture (BMDCs)

Bone marrow-derived dendritic cells (BMDCs) from 8–10-week-old C57BL/6 mice (Charles River) were obtained by carefully removing the femur and tibia of mouse legs using forceps and scissors and transferring to ice-cold media. The bones were then soaked in ethanol for 15 seconds then rinsed with Phosphate Buffered Saline (PBS, Gibco). Each bone was cut above and below each joint and flushed with cell culture media using a 25G needle on a falcon tube. The solution was centrifuged at 1500rpm for 3:30 min, and cells were resuspended in 3mL of ACK lysing buffer (Gibco) for 30 sec. Cells were centrifuged a second time at 1500rpm for 3:30min, resuspended in 1ml

medium and filtered using a 70µm Nylon mesh (Falcon) before counting the cells. Cells were then cultured in RPMI1640 with L-glutamine and sodium bicarbonate (Sigma-aldrich) supplemented with 10% Fetal Bovine Serum (FBS, Gibco), 20ng/ml recombinant murine GM-CSF (Peprotech), 1% anti-anti (Gibco) and 55uM 2-Mercaptoethanol (Gibco) at 37C with 5% $CO_2$. Exposure to the stimulatory factor and cell activation were optimized and achieved through patent-pending methodology.

*Exposure to whole tumor /SIINFEKL antigens:* cells recovered on day 8 were plated at a density of $1X10^6$ cells per well using 6-well plates in a final volume of 5ml of RPMI1640 with L-glutamine and sodium bicarbonate supplemented with 10% exosome-free FBS (Gibco), 1% anti-anti and 1:1 ratio of whole tumor antigen or 100ug/ml of SIINFEKL peptide (ovalbumin, IBA lifesciences) at 37C with 5% $CO_2$ for 24H.
After incubation for 24H at each condition, the detached cells were recovered and used for protein extraction in western blot analysis, exosome isolation, or saved in -80C using cell freezing medium-DMSO 1X (Sigma) for downstream applications.

### 2.1.2. Whole-tumor Antigen Preparation

A solution of 2mg/ml of Collagenase from Clostridium histolyticum (Sigma) was made in High Glucose Dulbecco's Modified Eagle medium (HG-DMEM) (Sigma) supplemented with 10% (FBS), 5 µg/mL insulin, 5 µg/mL transferrin and 5 ng/mL sodium selenite (1× ITS, Sigma) and 1% anti-anti (Gibco). Tumor pieces obtained from ID8 injected female C57BL/6 mice (methods in section 3) were cut into small pieces and incubated in 5ml of collagenase at room temperature for 30 min. The solution was filtered through a 70µm Nylon mesh (Falcon) and centrifuged at 300xg for 14 min

before filtering through a new 70µm Nylon mesh and counting the cells. A 1:100 dilution of Sodium Hypochloride (NaOCl, Sigma-Aldrich)) was made in 1X PBS (Gibco) and 6/100 ratio of NaOCl to volume of cell sample was added and incubated for 1H at room temperature vortexing every 30 min. The solution was then centrifuged for 500xg for 5 min and washed twice with 0.22um filtered 1X PBS. This was followed by 6 8-minute freeze/thaw cycles and saved in -80C for downstream application.

### 2.1.3. Exosome Isolation

After 24H of exposure to whole tumor antigen, PIC or cell media alone, cells were centrifuged at 500 xg for 5 mins. Without disturbing cell pellet, media was transferred to clean tube for exosome extraction. The media was centrifuged at 2000 xg for 30 mins to pellet any remaining cell debris. The cell debris collected were stored using cell freezing medium-DMSO 1X (Sigma) and kept in -80C for downstream application while the supernatant was transferred to a clean tube and media was filtered with 0.22 um PES membrane filter (Celltreat scientific products). The filtered media was concentrated using 10 KDa (Amicon) ultra centrifugal filters and centrifuged at 4000 xg for 15 mins at 4C. The concentrate was transferred to a clean tube and total exosome isolation reagent (Invitrogen) was added at a 1:2 ratio of the recovered concentrate. The solution was mixed well by vortexing and was incubated overnight at 4C. The next morning, the solution was centrifuged at 10,000 xg for 1 hr at 4C. Without disturbing the pellet, the supernatant was discarded, and the pellet was resuspended in 0.22um filtered 1X PBS (Gibco) before storing at -80C for use in downstream applications.

### 2.1.4. Nanoparticle Tracking Analysis

The NS300 Nanosight System (Malvern) was used to determine size and concentration. A 200X dilution in filtered phosphate buffered solution (PBS) was prepared for each sample. Four videos of 60 seconds each were recorded for each sample using NTA 3.0 software, and the threshold was kept constant at 8.

### 2.1.5. Western Blot

Protein extraction of Dex was achieved by resuspending the pellet in 100ul of lysis buffer (M-PER™ Mammalian Protein Extraction Reagent (ThermoFisher) and 1X of Protease & Phosphatase inhibitors 100X (ThermoScientific)). Samples were prepared using 50ug of protein, 6ul loading buffer (1 in 20 5% mercaptoethanol (Gibco) and LDS sample buffer non reducing 4X (ThermoScientific)) and M-PER™ Mammalian Protein Extraction Reagent (ThermoFisher) to a final volume of 24ul and loaded into Mini Protean TGX precast gels (BioRad). The electrophoresis system was run at 80V for 30min then 120V at room temperature until samples reached the bottom of the gel. The gel was then transferred onto Amersham Protran blotting membrane (0.1um, GE Healthcare Lifescience) and blocked using 5% BSA (Cell Signaling Technology) in 1X TBST (20X AMRESCO) for 1 hr at room temperature with shaking. Anti-Alix (Santa Cruz Biotechnologies), Anti-TSG-101 (abcam) or Anti-CD-9 (abcam) were added, and membrane incubated overnight at 4C with shaking. The membrane was washed with 1X TBST for 5min 3 times before incubating with the secondary antibody for 45min at room temperature under shaking. The wash was repeated, and proteins detected using SRX-101A tabletop processor (Konica Minolta).

### 2.1.6. Exosomal suspension preparation

Dex membranes were stained using PKH26GL Red Fluorescent Cell Linker Kit (Sigma) to be able to clearly identify exosomes through ImageStream and flow cytometry using the manufacturer's instructions. Briefly, 350ul exosomes were added to 1ml of Diluent C and this suspension was added to 2X dye solution and incubated for 5 min at room temperature (RT). Following the incubation, equal amounts of exosome-free FBS (Glibco) were added to the solution and incubated for an additional minute at RT before washing. Washes were performed by ultracentrifuging mixture at 40000xg for 1hr at 4°C. The pellet recovered was resuspended in 1ml of 0.22um filtered PBS (Gibco) and exosome spin columns (MW3000, Invitrogen) were used to remove any unbound dye.

**2.1.6.1.** ***Exosome conjugation to beads*** After being stained, exosomes were conjugated with Aldehyde/Sulfate Latex Beads (ThermoFisher). To optimize the protocol, different beads:exosome:beads ratios (1:100, 1:500 and 1:1000) were tested. Conjugation occurred for 15 min at room temperature RT under shaking. Consequently, 0.22um filtered 1X PBS was added to 1 ml final volume, and the samples were incubated overnight at 4C under shaking. The solution was briefly vortexed, and a 100 mM glycine solution (Sigma) was then added to saturate unbound beads and suspensions were incubated for 30 min under shaking at RT before centrifugation for 5min at 4000 rpm occurred. Exosomal samples were subsequently analyzed by flow cytometry and ImageStream.

### 2.1.7. Image Stream analysis

Image data was acquired on an Amnis ImageStream$^{x}$ (Luminex Corporation) using the x60 magnification option. Analysis of the sample data for comparison with standard Flow Cytometry data identified single beads with a Brightfield Area vs Darkfield Intensity gate, from which was generated a fluorescence Intensity histogram. The analysis for Figure 6 identified single beads with a Brightfield Area vs Brightfield Aspect Ratio gate, from which was generated a Brightfield Gradient RMS histogram. Visual validation was used to set an "in focus" gate. All subsequent analysis was conducted on the single & focused population.

Punctate vs Diffuse staining patterns (Figure 6) were established using a Morphology (M03_Ch03) mask to identify the PKA stained area and then gating using a Symmetry 3_Morphology(M03_Ch03) vs Major Axis Intensity_Morphology(M03_Ch03) plot. High Symmetry 3 values equated to a punctate staining profile.

All gating strategies and analytical pathways were confirmed by visual validation of the populations generated

**2.1.8. <u>Flow cytometry analysis</u>**

**2.1.8.1. <u>*For cell analysis:*</u>** Briefly, 1X10$^{6}$ DC-control, DC-PIC and DC-PO were counted and checked for viability using trypan blue stain (Thermofisher) and divided into 5ml FACS tubes (Falcon). A cocktail of PerCP/Cy5.5-anti-mouse CD80 (biolegend), PE-anti-mouse CD86 (biolegend), APC-anti-mouse MHCII (tonbo biosciences) and FITC-anti-mouse CD11c (biolegend) or PE anti-mouse OVA 257-264 SIINFELK peptide alone (invitrogren) was used at the concentration of 1:200. Cells were incubated in the dark for 30 min on ice. Cells were washed with 0.22um filtered

2% FBS and centrifuged were centrifuged at 500xg for 4 min at 4°C. Flow cytometry samples were acquired on Fortessa flow cytometer (Becton Dickinson) gating $5X10^3$ events on morphological plot (FCS vs SCS).

**2.1.8.2.** ***For exosome analysis:*** Flow cytometry samples were obtained using Fortessa flow cytometer (Becton Dickinson) gating $1X10^8$ events on PKH positive gate.

## 2.2. RESULTS

After inducing hematopoietic cells toward a dendritic cell lineage, flow cytometry analysis was used to quantify surface receptors in the three experimental groups ensuring adequate differentiation. Two populations of dendritic cells exist in our cell isolates, showing heterogeneous activation in all markers except the DC-specific marker CD11c confirming proper differentiation. Figure 1a shows that as cells are treated with adjuvant (Activated cells= DC-A) and are presented antigen (Activated + Ovalbumin= DC-AO), there is a shift from medium intense stained cells to highly stained cells highlighting the success in DC activation despite heterogeneity. Moreover, there is a step-wise increase in co-stimulatory markers as the DCs are incrementally exposed to adjuvant (A) or adjuvant and ovalbumin (AO) together (Figure 2a). There is also an increased percentage of CD80+CD86+ DCs after the cells are activated and presented antigen (Figure 2).

DC exosomal isolates (Dex) were processed using Nanosight Tracking Analysis (NTA) to quantify the concentration obtained and measure the size to ensure the vesicles obtained were within the allowed parameters by the ISEV (30-150nm).[4] The three experimental groups had size (nm) ranging from 90-110nm proving our vesicles were

exosomes (Figure 3a). The concentrations of Dex (part/ul) produced by one million DC were quantified with the NTA and no differences were noted in exosomal production between groups (Figure 3b).

The levels of protein expression between the Dex experimental groups were qualified using western blot analysis and found to be consistently expressed despite different levels of activation (Figure 4). Both membrane and fusion exosomal proteins, Alix and TSG 101 and CD9 respectively, were expressed by our exosomal isolates.

Lastly, since exosomes are direct invaginations of their progenitor cells, we expect the exosomes produced from DC will retain the markers necessary for T cellular activation. We began the project using bead-assisted flow cytometry to qualify and quantify the surface receptors of the Dex recovered but were met with several obstacles such as bead aggregation and the inability to localize our exosomes using fluorescent conjugated receptor antibodies since the aldehyde beads would absorb the dye, leading to inaccurate results. Taking advantage of the ImageStream software features, we were able to eliminate background noise and increase the sensitivity of bead-assisted flow cytometry to accurately measure exosomal markers increasing sensitivity and accuracy of results for quality control of exosomal preparations.

We analyzed our samples using the ImageStream (Figure 5a) followed by flow cytometry analysis of the sample sample (Figure 5b). This was achieved by staining Dex using PKH fluorescent dye and conjugating to aldehyde beads at three different concentrations to optimize sample ratios. In both platforms, we find that maximum saturation is achieved at 1:500 and, through the morphological plot, are able to visualize

the different populations of beads representing doublets, singlets and aggregates that are present when analyzing through bead-based flow cytometry. Figure 5c shows that the two platforms are comparable and similar results can be obtained when looking only at fluorescence.

Furthermore, the use of the mask feature in the ImageStream platform, allowed us to select single beads and visualize the staining pattern of the exosomes to ensure accurate quantification. Figure 6a shows the gating of single beads and further selection of diffuse vs punctate staining. Figure 6b shows a representative image of the aldehyde beads with single (punctate) and multiple beads (diffuse) on its surface. When comparing the three different ratios of beads: exosomes, 6-15% of the measured events had single beads on their surface.

This method was useful in removing errors associated with flow cytometry when attempting to quantify exosomal receptors due to issues previously discussed such as fluorescence absorbance by the bead, bead aggregation, and failure to quantify single exosome fluorescence – issues that are solved with the combined power of microscopy and flow cytometry analysis of the ImageStream.

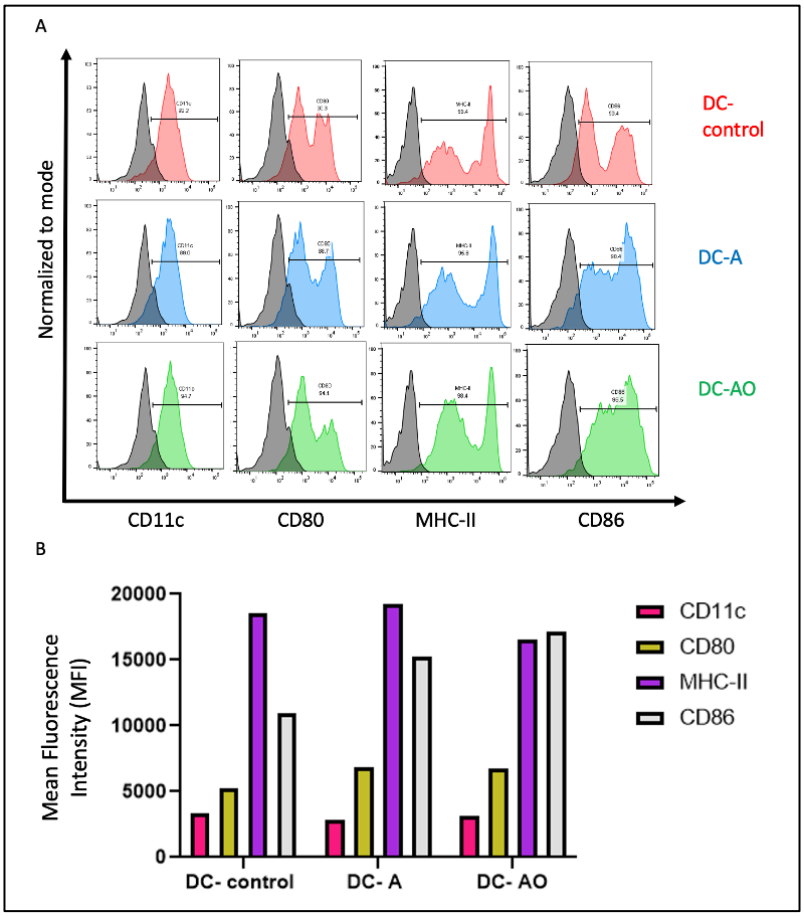


**Figure 1. Flow cytometry data for DC-specific markers (CD11c), antigen-presenting markers (MHCII), and co-stimulatory markers (CD86 and CD80). A) Hystographical representation of cell markers present in three different experimental conditions DC-control (red), DC-Activated (DC-A, blue), DC-Activated/Ovalbumin (DC-AO, green) with data normalized to mode. B) Surface receptor expression is represented as mean fluorescence intensity (MFI).**

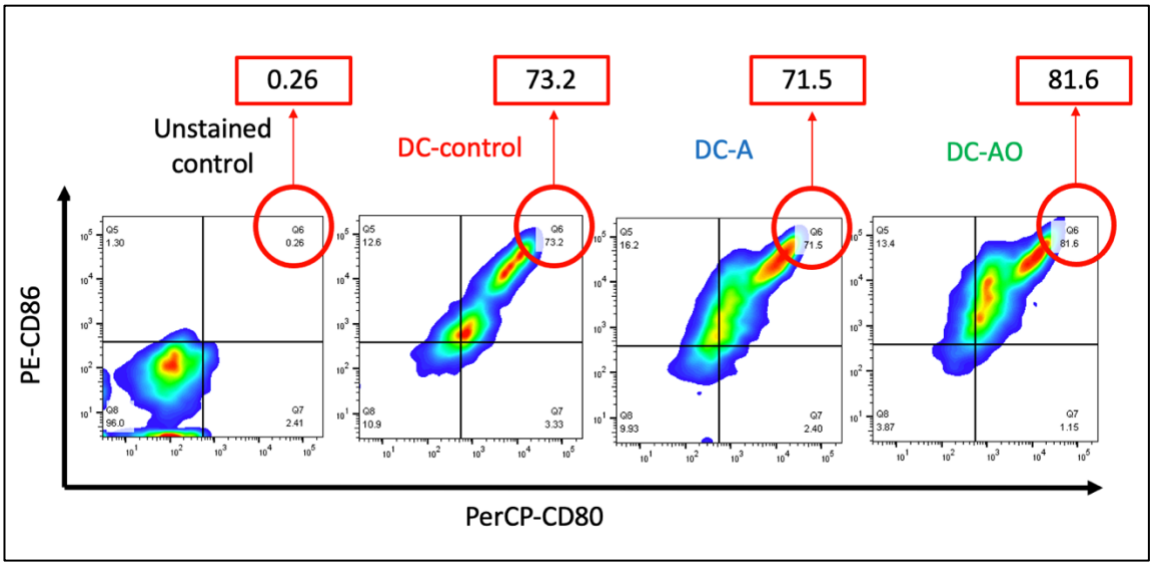


**Figure 2. Identification maturity looking at CD86+CD80+ dendritic cells.**

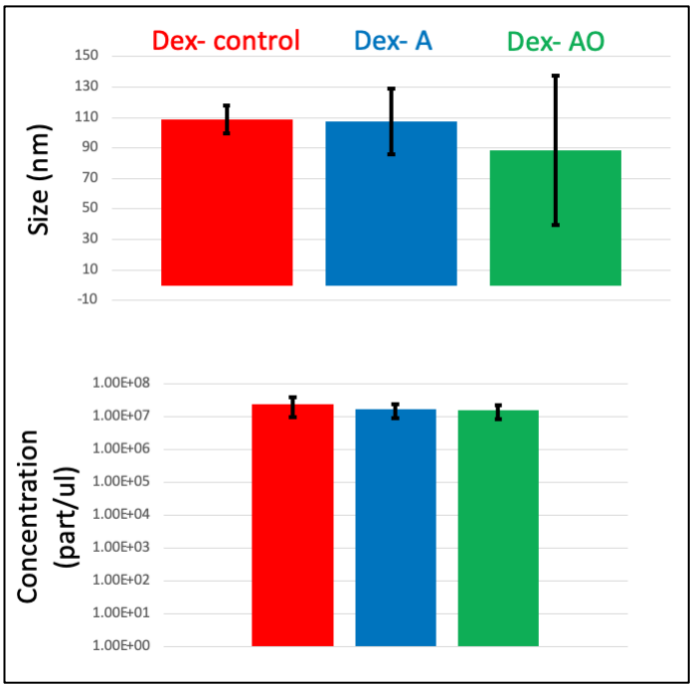


**Figure 3. Nanoparticle Tracking Analysis (NTA) showing size (nm) and concentration (part/ul) of exosomes produced by one million cells.**

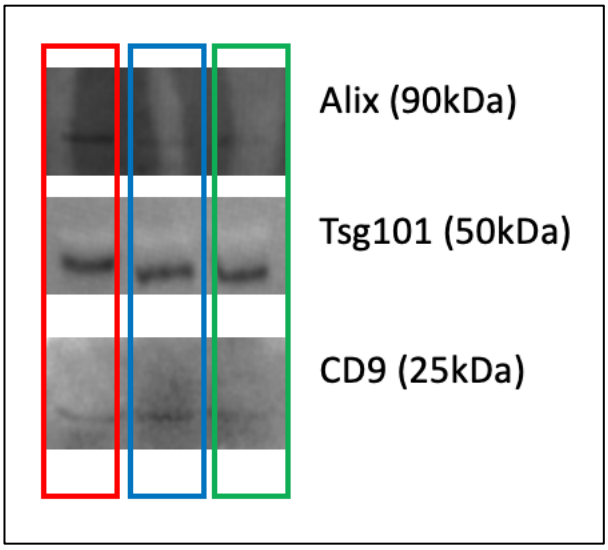


**Figure 4. Dex control (red), Dex-A (blue) and Dex AO (green) protein expression of membrane and fusion proteins (Alix, TSG101, CD9).**

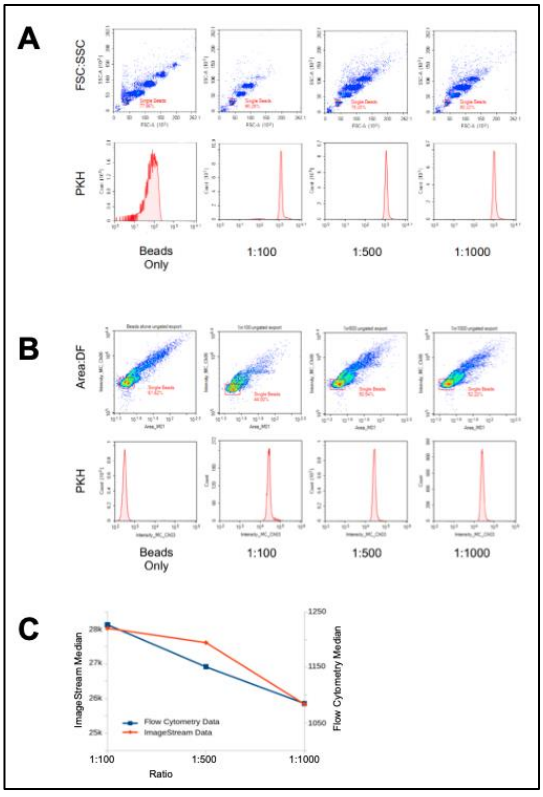


**Figure 5. Comparison of Flow Cytometry data with ImageStream data from same samples using three different beads to exosomes ratios. A) Flow Cytometry data of**

**various ratios – both FSC:SSC and PKH staining. B) ImageStream data of various ratios exported to FCS files for analysis – both BF Area:DF and PKH staining. C) Comparison of PKH staining across ratios assessed by both analysis platforms.**

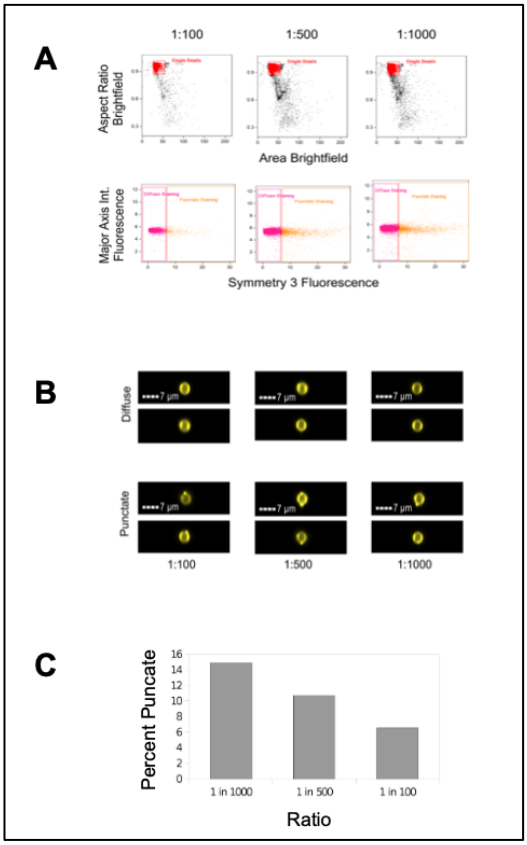


**Figure 6. Identification of different exosome binding patterns. A) Automatic identification of single beads and those expressing a punctate stain vs a diffuse stain. B) Representative images of PKH stained exosome beads. C) Percentage of beads identifying as "punctate stained" for each bead:exosome ratio**

## 2.3. REFERENCES


1. Metlay, J. P., Witmer-Pack, M. D., Agger, R., Crowley, M. T., Lawless, D., & Steinman, R. M. (1990). The distinct leukocyte integrins of mouse spleen dendritic cells as identified with new hamster monoclonal antibodies. *Journal of Experimental Medicine, 171*(5), 1753–1771. https://doi.org/10.1084/jem.171.5.1753

2. Fuertes Marraco, S. A., Grosjean, F., Duval, A., Rosa, M., Lavanchy, C., Ashok, D., Haller, S., Otten, L. A., Steiner, Q.-G., Descombes, P., Luber, C. A., Meissner, F., Mann, M., Szeles, L., Reith, W., & Acha-Orbea, H. (2012). Novel murine dendritic cell lines: A powerful auxiliary tool for Dendritic Cell Research. *Frontiers in Immunology*, *3*. https://doi.org/10.3389/fimmu.2012.00331

3. Théry, C., Witwer, K. W., Aikawa, E., Alcaraz, M. J., Anderson, J. D., Andriantsitohaina, R., Antoniou, A., Arab, T., Archer, F., Atkin-Smith, G. K., Ayre, D. C., Bach, J.-M., Bachurski, D., Baharvand, H., Balaj, L., Baldacchino, S., Bauer, N. N., Baxter, A. A., Bebawy, M., … Zuba-Surma, E. K. (2018). Minimal information for studies of extracellular VESICLES 2018 (MISEV2018): A position statement of the International society for Extracellular vesicles and update of the Misev2014 guidelines. *Journal of Extracellular Vesicles*, *7*(1), 1535750.

4. Cheng, L., Wu, S., Zhang, K., Qing, Y., & Xu, T. (2017). A comprehensive overview of exosomes in ovarian cancer: Emerging biomarkers and therapeutic strategies. *Journal of Ovarian Research, 10*(1). doi:10.1186/s13048-017-0368-6

5. Théry, C., Witwer, K. W., Aikawa, E., Alcaraz, M. J., Anderson, J. D., Andriantsitohaina, R., Antoniou, A., Arab, T., Archer, F., Atkin-Smith, G. K., Ayre, D. C., Bach, J.-M., Bachurski, D., Baharvand, H., Balaj, L., Baldacchino, S., Bauer,

N. N., Baxter, A. A., Bebawy, M., … Zuba-Surma, E. K. (2018). Minimal information for studies of extracellular VESICLES 2018 (MISEV2018): A position statement of the International society for Extracellular vesicles and update of the Misev2014 guidelines. *Journal of Extracellular Vesicles, 7*(1), 1535750. https://doi.org/10.1080/20013078.2018.1535750

6. Suárez, H., Gámez-Valero, A., Reyes, R., López-Martín, S., Rodríguez, M. J., Carrascosa, J. L., Cabañas, C., Borràs, F. E., & Yáñez-Mó, M. (2017). A bead-assisted flow cytometry method for the semi-quantitative analysis of Extracellular Vesicles. *Scientific Reports, 7*(1). https://doi.org/10.1038/s41598-017-11249-2

# 3. ASSESSMENT OF T-CELL ACTIVATION

Immunotherapy involves using the body's own immune system to attack malignant cells and provides a personalized treatment strategy for patients to get targeted results that avoid many of the side effects seen with chemotherapy and radiation.[1] It takes advantage of the ability of these antigen-presenting cells (APCs) to activate cytotoxic T cells and attack a specific tumor usually by pulsing the cells with a peptide that is common to a specific type of cancer or using a cocktail of antigens that can be displayed all at once to the cell. [2,3].

Following the isolation of exosomes for DCs, we needed to ensure there was proper antigen processing to be able to activate immune cells against the targeted cancer protein cocktail. Here, we measure adequate T-cell activation by looking at cytokine "IFN-gamma" expression and cell proliferation as measures of cytotoxic T-cell stimulation.

## 3.1. METHODS

### **3.1.1. Naïve CD8+ T Cell Culture**

Splenocytes were obtained from OT-1 mice (Charles River) by slicing the excised spleen and placing the fragments through a 70um strainer (Falcon) using the plunger end of a syringe attached to a 50-mL conical tube. The cells were washed through the strainer with 1X PBS (Gibco) and centrifuged at 1600rpm for 5 minutes. The cell pellet was resuspended in 3 mL ACK lysing buffer (Gibco) for 1 minute and 30 ml of PBS were added. The cells were centrifuged at 1600rpm for 5 minutes and cells were resuspended in 2% exosome-free FBS (Gibco) at a concentration of $1X10^8$/ml and manufacturer's

protocol was followed to obtain Naïve CD8+ population (Naïve CD8+ T cell isolation kit, STEMCELL technologies).

### 3.1.2. CFSE Cell Staining

A 5uM working concentration of CellTrace CFSE dye (Invitrogen) was prepared according to the manufacturer's protocol by adding 18ul of DMSO to the dye solution. A cell suspension of Naïve CD8+ T cells was prepared in 1X PBS and 1ul of CFSE was added per ml of cell suspension. The solution was then incubated for 20 min at 37°C in a dark environment. Culture media (RPMI1640 with L-glutamine and sodium bicarbonate (Sigma-aldrich) supplemented with 10% exosome-free FBS (Gibco), 20ng/ml recombinant murine GM-CSF (Peprotech), 1% antibiotic-antimycotic (Anti-Anti, Gibco) and 55uM 2-Mercaptoethanol (Gibco)) was added at five times the amount of the stained cell suspension and incubated for 5 min at 37°C.[4,5] The cells were then centrifuged at 450xg for 5min and resuspended at a concentration of $1.5X10^6$ cells/ml in culture media.

### 3.1.3. In-vitro T-cell stimulation assay

CFSE-stained Naïve CD8+ T cells in a $1.5X10^6$ cells/ml concentration were placed into a 96 well plate (Falcon) using 100ul aliquots. Aliquots of 100ul were used for each control and sample. Ovalbumin (100ug/ml) was used as a positive control; culture media as above was used as a negative control. Dex control, PIC treated, and PIC/ovalbumin treated were plated in quadruplicates at three different concentrations ($1X10^8$, $5X10^8$, $1X10^9$ exosomes/ml). Suspended cells were recovered after 3 days of incubation at 37°C with 5% $CO_2$ and placed in round-bottom polypropylene tubes.[6] Cells were centrifuged at 500xg for 5 min and fixed while the media was saved in -20°C for ELISA.

### 3.1.4. Sample fixation

Cells were pelleted at 500xg for 5 min at 4°C and washed with 0.22um filtered 1% FBS (Gibco). Afterwards, cells were fixed using 0.22um filtered 1% formaldehyde for 15min on ice. Cells were washed for a second time using 0.22um filtered 1% FBS and centrifuged at 500xg for 5 min at 4°C before resuspending in 0.22um filtered PBS.

### 3.1.5. Flow cytometry analysis

Flow Cytometry samples were acquired on a Fortessa flow cytometer (Becton Dickinson). Gating $1X10^4$ events on the morphological plot (FCS vs SCS).

### 3.1.6. IFN-gamma ELISA

Reagents, standard dilutions, and samples from the in-vitro T cell stimulation were prepared as directed by the manufacturer's instructions for the mouse IFN-gamma quantikine ELISA kit (R&D Biosystems). Assay diluent (50ul) was added to each well followed by 50ul of each standard and control in triplicates and samples in quatriplicates. The plate was sealed and incubated at room temperature for 2 hours. The plates were washed for a total of 3 washes using an automatic plate washer before 100ul of conjugate were added to each well and incubated at room temperature for an additional 2 hours. The plate washing was repeated for a total of 3 washes. A total of 100ul of substrate solution was added to each well and the plate was incubated for 30 minutes at room temperature in the dark. Following the incubation period, 100ul of stop solution were added to each well. The plate was read at 450nm using Synergy H4 hybrid reader (biotek).

### 3.1.7. Statistical analysis

Statistical analysis was performed by unpaired t-test using GraphPad Prism. Data with a $P < 0.05$ were considered significant ($*P < 0.05$, $**P < 0.01$, $***P < 0.001$, $****P<0.0001$).

## 3.2. RESULTS

Splenocytes from transgenic T cell receptor mice (OT-1) were used to determine if Dex processed and presented antigen as they are designed to recognize the ovalbumin residue. Dex control, A and AO were plated at three different concentrations (data not shown) and incubated for three days to ensure proper stimulation.[6] The $1X10^9$ concentration over-stimulated the CD8+ T cells and peaks from cell division were not able to be appreciated. Figure 7a shows 5 different peas meaning 5 cell divisions occurred from the time the cells were exposed to the antigen-presenting exosomes. Our data shows that consequently, as higher concentrations of exosomes are used, greater stimulation occurs leading to more immune activation. As the cells divide, the cell membrane dye begins to dilute, causing a lower mean fluorescence intensity to be detected (figure 7b). Dex AO significantly increased the proliferation rate of CD8+ T cells when compared to our negative control.

After establishing Dex processed and presented antigen similarly to their progenitor cells, we ensured the T cells were signaling other immune cells to further promote the attack of the antigen they were being shown. Dex AO significantly

improved the IFN-gamma cytokine levels produced from CD8+ T cells when compared to background levels alone.

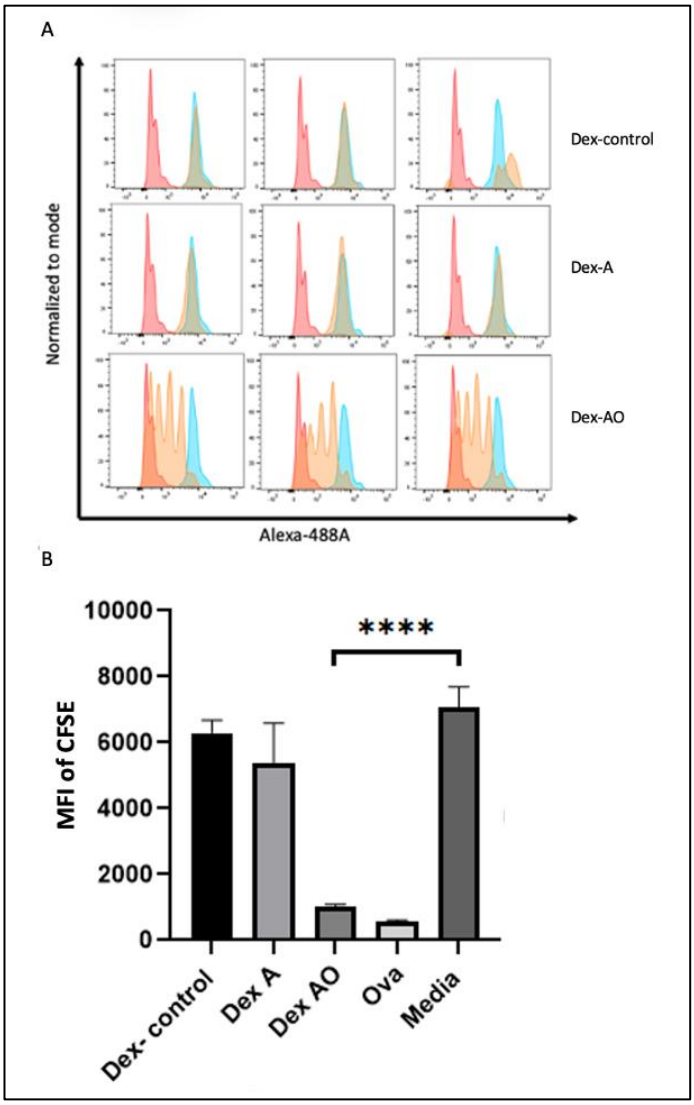


**Figure 7. Antigen processing studies using CFSE cell trace methodology. A) CD8+ T cell division assessed by the number of peaks (orange). Ovalbumin (100ug/ml) was used as a positive control (blue) while media was used as a negative control (red). B) CFSE dye dilution measured by mean fluorescence intensity (MFI). (****;p<0.0001)**

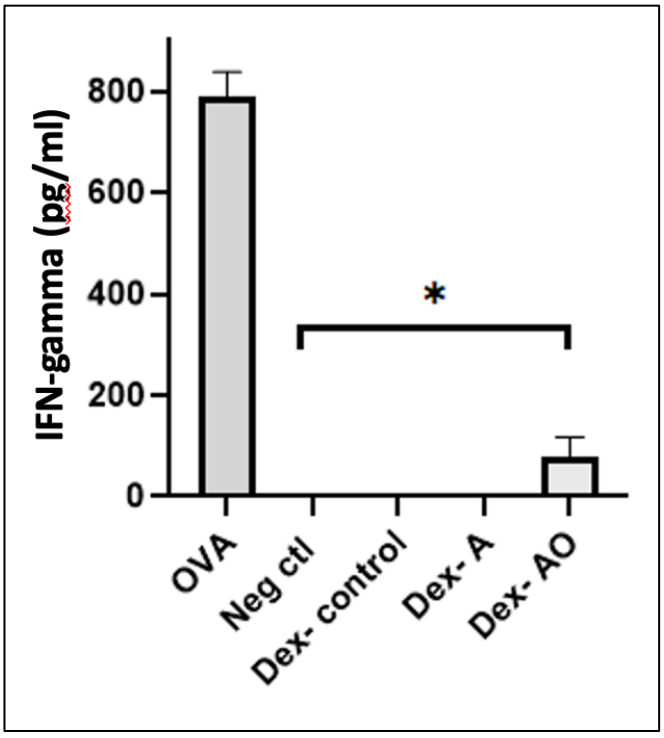


**Figure 8. Interferon-gamma expression (pg/ml) of CD8+ T cells exposed to Dex. 100ug/ml of ovalbumin were used as a positive control and media was used as a negative control. A total of $1X10^9$ exosomes/ml were used per condition. (*;p<0.05)**

3.3. REFERENCES

1. Gaillard, S. L., Secord, A. A., & Monk, B. (2016). The role of immune checkpoint inhibition in the treatment of ovarian cancer. *Gynecologic Oncology Research and Practice, 3*(1). doi:10.1186/s40661-016-0033-6

2. Liu M, Guo F. Recent updates on cancer immunotherapy. *Precis Clin Med.* 2018;1(2):65-74. Doi:10.1093/pcmedi/pby011

3. Chen, S., Lv, M., Fang, S., Ye, W., Gao, Y., & Xu, Y. (2018). Poly(I:C) enhanced anti-cervical cancer immunities induced by dendritic cells-derived exosomes. *International Journal of Biological Macromolecules, 113*, 1182-1187. doi:10.1016/j.ijbiomac.2018.02.034

4. Chang MP et al. *Requirement of 2-mercaptoethanol for in vitro growth factor production by T cells and vulnerability of the response to age.* Mech Ageing Dev. 1982 Sep;20(1):65-73.

5. Burger M et al. *The role of 2-mercaptoethanol in the stimulation of spleen cell cultures: increased uptake of cystine into the TCA-soluble pool.* Immunol Lett. 1982 Apr;4(4):193-7.

6. Elvin et al. Protection against Heterologous *Burkholderia pseudomallei* Strains by Dedritic Cell Immunization. American Society for Microbiology. DOI: 10.1128/IAI.74.3.1706-1711.2006

# 4. BIODISTRIBUTION OF EXOSOMES

Ovarian cancer is the eight most commonly occurring malignancy affecting women worldwide. Epithelial ovarian cancer (EOC) comprises most of these diagnoses. Most women experience vague symptoms and are diagnosed at advanced stages of the disease and, despite optimal treatment, up to 85% of them will relapse. Multiple clinical trials are testing the benefits of immunotherapeutics as co-adjuvants in the treatments of ovarian cancer patients. Dendritic cell-derived exosomes (Dex) represent an attractive alternative to existing immunotherapeutic approaches, due to their nanoscopic size and ability to enter cells without the need of receptors. However, no clinical trials currently exist testing dendritic cells derivatives in ovarian cancer. Therefore, we aimed to compare the biodistribution of Dex when injected through various treatment routes in a mouse model of epithelial ovarian cancer in an effort to better understand how they affect the bioavailability of exosomes after delivery.

## 4.1. METHODS

### 4.1.1. **Cell line**

The ID8 cell line, originated from mouse ovarian surface epithelial cells (MOSEC), was purchased from Merck-Millipore. Cells were cultured in High Glucose Dulbecco's Modified Eagle medium (HG-DMEM) (Sigma) supplemented with 10% fetal bovine serum (FBS, Gibco), 5 μg/mL insulin, 5 μg/mL transferrin and 5 ng/mL sodium selenite (1× ITS, Sigma) and 1% Anti-anti (Sigma) at 37°C with 5% $CO_2$.[1]

### **4.1.2. Ovarian cancer tumor model-ID8 tumor growth**

Female 8–10-week-old C57BL/6 mice were injected intraperitoneally with $1 \times 10^7$ ID8-GFP cells in 200 μL of PBS. Cells were injected into the lower right quadrant of the abdomen.[1] Mice weights (g) were recorded weekly after the injection and images of animals, tumors and ascites development were taken with a smartphone camera. All animal studies were carried out in accordance with guidelines determined by the Animal Welfare Act and the Guide for the Care and Use of Laboratory Animals and complied with protocols approved by the Institutional Animal Care and Use Committee at the Houston Methodist Research Institute (AUP-0219-0013).

#### 4.1.3. Visualization of tumor growth

Briefly, 200 μL of 15 mg/mL D-luciferin was injected into the mice's abdomen and the bioluminescent signal was evaluated after 10 min for peak signal emission using Xenogen IVIS Spectrum imaging system (PerkinElmer). The signal was quantified using the Living Image software (PerkinElmer) starting at day 0 after tumor cell injection. Images were normalized using the Living Image software (PerkinElmer).[1]

#### 4.1.4. Exosomal membrane staining with DiD

Briefly, $8X10^9$ Dex-control were obtained before mixing with 2.1ul of Vybrant DiD Cell-labeling solution (Invitrogen). The exosomal solution was mixed and incubated for 20 minutes in the dark at room temperature. Following the incubation, unbound dye was removed by using exosome spin columns (3000MW, Invitrogen) following manufacturer's protocol.

#### 4.1.5. Exosomal distribution visualization

A hundred and six days after epithelial ovarian cancer cell injection with $1X10^7$ ID8-GFP, a portion of the mice began developing ascitic fluid. Ascites development was determined by visual inspection and palpation as well as weight tracking. Mice were divided into three groups: tumor-bearing mice with ascites (group 1, n=4), tumor-bearing mice without ascites (group 2, n=4), and a control group (group 3, n=4). A total of $8X10^9$ Dex-control stained with DiD cell-labeling solution were injected intraperitoneally to group 1 while groups 2 and 3 received an intravenous injection. Signal was read at 0, 4, 8 and 24 hours at an excitation of 644nm and emission of 655nm using Xenogen IVIS Spectrum imaging system (PerkinElmer). Mice were sacrificed at given time points and peritoneal membrane, liver, heart, lungs, kidneys, lymph nodes, tumor nodules and ascitic fluid were collected and DiD signal read as above. Tissues were saved using OCT compound (Tissue-Plus) and stored in -80C for future studies.

## 4.2. RESULTS

Ten female C57BL/6 mice were injected with $1X10^7$ ID8-GFP cells intraperitoneally and tumor growth was monitored through weekly weights and IVIS Spectrum imaging. Tumor signal was first noticed around day 30 and can be seen growing within the peritoneal cavity signaling tumor growth (Figure 9). High-intensity signals such as the one being pointed by the red arrow in figure 9, were seen when the mice were starting to develop ascites. Intraperitoneal injection (IP) of fluorescently-labeled exosomes showed that at 24 hours, Dex are found concentrated at the tumor bulk (Figure 10b). Unfortunately, no exosomes were found within the tissues or tumor bulk 24 hours post IP injection (Figure 10c). In fact, even with the extraction of the ascitic

fluid, imaging of the mice and ascites found that no exosomes could be visualized by fluorescence signaling at the 24 hours mark (Figure 11). Studies with intravenous injection showed heterogeneous results within the different groups, but two things that remained the same were the exosomal processing by the liver and the accumulation of the exosomes in the spleen. The latter could mean that the exosomes could have more time to present antigen to other immune cells if administered via this route (Figure 12). Similar to IP injection, IV injection to tumor-bearing mice showed some involvement of the tumor bulk 24 hours post injection (Figure 12b). Interestingly enough, the tumor bulk is not the only area the exosomes gathered at 24 hours post injection outside of the liver and spleen. Figure 12d shows one renal lymph node with a red spec (blue arrow) representing exosomes traveling to the area.

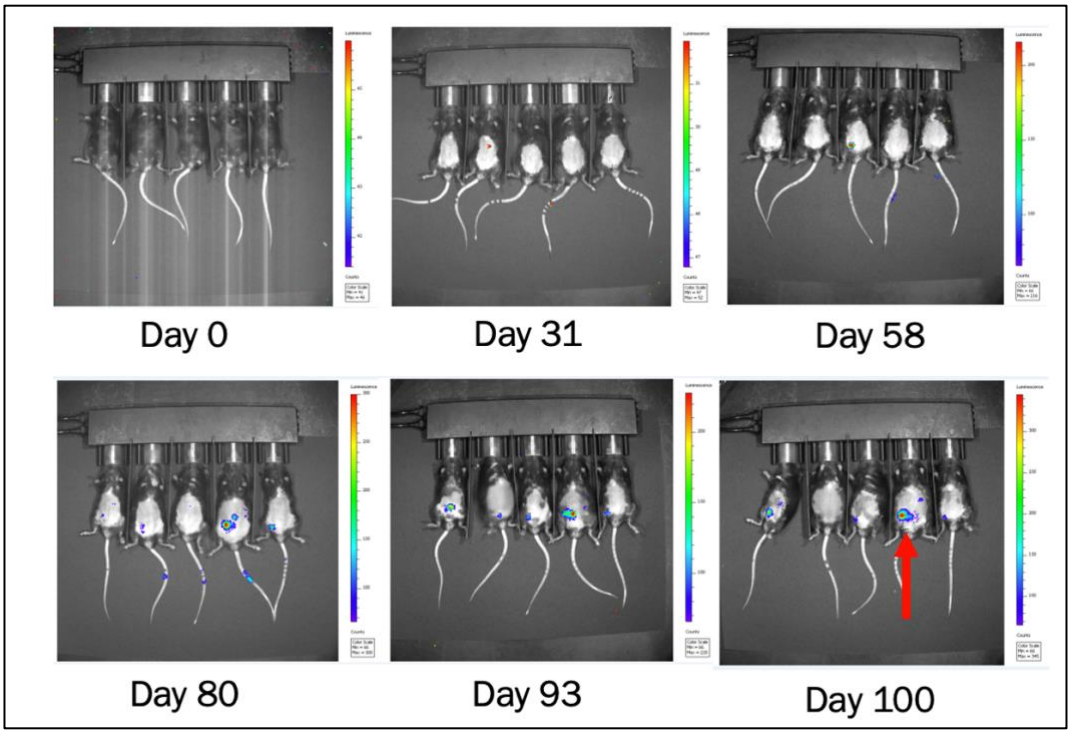


**Figure 9. Representative image of female C57BL/6 mice tumor growth visualization. 1X10$^7$ ID8-GFP cells were injected intraperitoneally to each mouse and growth was acessed weekly using luciferase to visualize the tumor cells through the In Vitro Imaging System (IVIS). The red arrow points to a high-intensity signal in the mouse abdomen indicating tumor growth in the animal.**

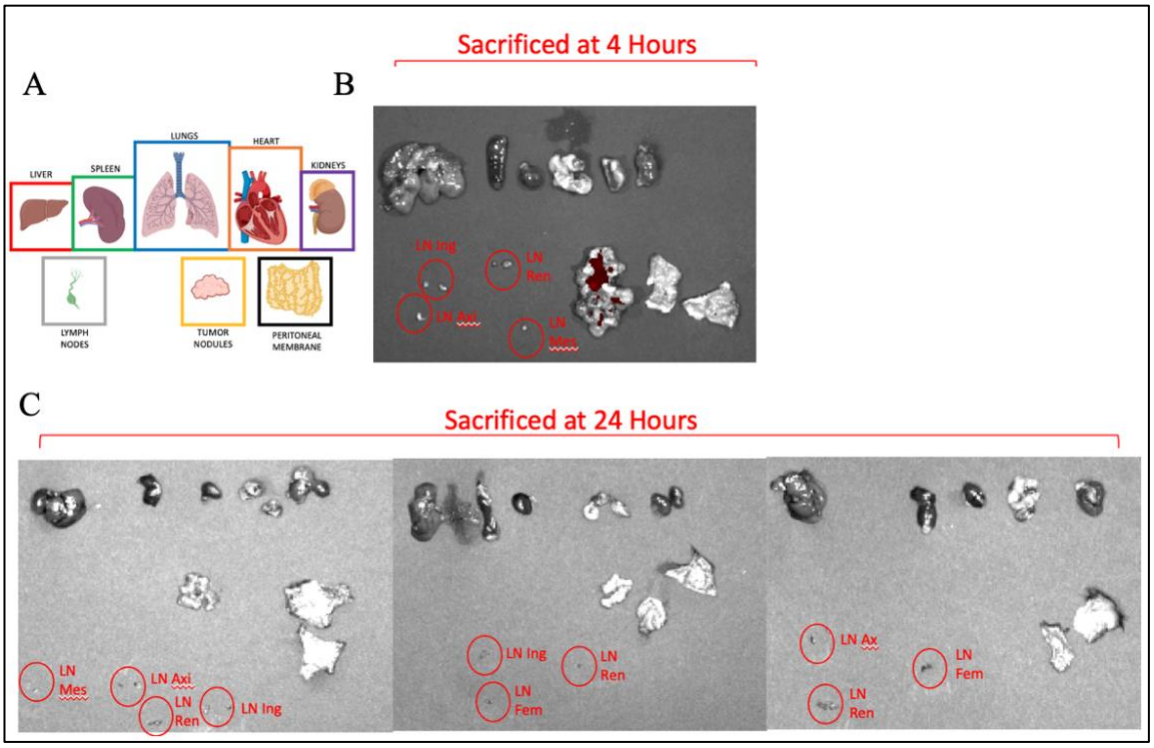


**Figure 10. Exosomal biodistribution after intraperitoneal injection (IP). A) Representative image of tissues recovered after mouse sacrifice 4 hours (B) and 24 hours (C) post IP injection.**

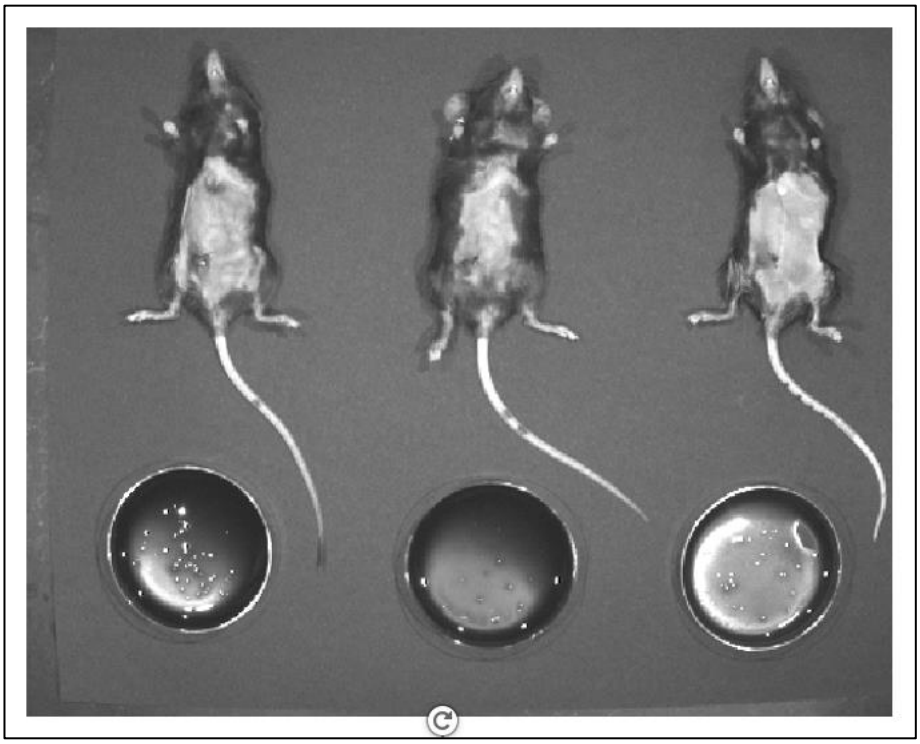

**Figure 11. Ascites recovered 24 hours after intraperitoneal injection with Dex-DiD.**

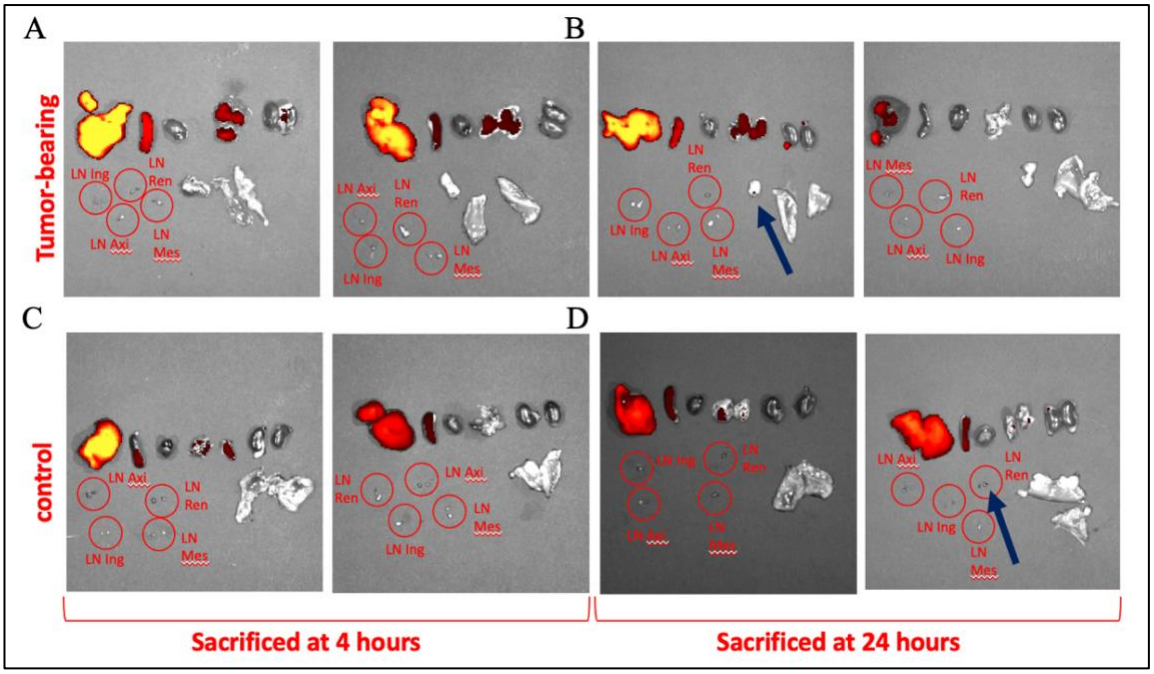


**Figure 12. Exosome distribution after intravenous injection (IV). A) Tumor-bearing mice without ascites sacrificed at 4 hours and 24 hours (B) post IV**

**injection. C) Control mice sacrificed at 4 hours and 24 hours (D) post IV injection. Blue arrows pointing slight red pigmentation in the tissue signifying the presence of exosomes. (Organ distribution similar to representative image in figure 10a).**

## 4.3. REFERENCES

1. Pisano, S., Lenna, S., Healey, G. D., Izardi, F., Meeks, L., Jimenez, Y. S., Velazquez, O. S., Gonzalez, D., Conlan, R. S., & Corradetti, B. (2021). Assessment of the immune landscapes of advanced ovarian cancer in an optimized in vivo model. *Clinical and Translational Medicine*, *11*(10). https://doi.org/10.1002/ctm2.551

# 5. CONCLUSIONS

The challenge in creating a powerful immunotherapeutic vaccine was to produce exosomes that would not only share the same receptor activation we saw in the cellular counterparts but also be capable of activating the immune system. We developed highly immunogenic dendritic cells based on their levels of CD80 and CD86 co-stimulatory markers.

DCs pulsed with ovalbumin produced exosomes that were capable of presenting the antigen resulting in increased T-cell proliferation. Dex were also able to induce INF-gamma expression, creating an environment suitable for further immune activation and signaling with the use of the cytokine when Dex were activated and presented antigen (Dex-AO)

Lastly, we showed for the first time in an ovarian cancer model, where Dex travel to when injected both intraperitoneally and intravenously. The information obtained allows us to speculate that IP treatment with Dex is short-lived and would require us to use high concentrations in our vaccinations for future studies. IV injection is processed by the liver and spleen and Dex would be capable of presenting more immune cells with the antigen and would perhaps need a smaller concentration of exosomes compared to IP injections. This advantage of the IP treatment modality allows us to obtain more vaccinations from the same amount of DCs.

Future directions of the study include quantification of exosomal receptors using our optimized method of bead-assisted cytometry using ImageStream, comparing T-cell activation by exosome and cells, increasing the number of mice treated with intravenous

vs intraperitoneal injection to obtain statistics, and testing AO-WTA Dex injections in mice with ovarian cancer testing for decrease in tumor burden and progression-free survival using IVIS-CT imaging modalities.